



**Publisher: ISES**

## **Application of Seismic Refraction technique in estimation of bedrock depth for civil engineering constructions at a site in Andhra Pradesh**

*S. Trupti\*, P. Pavan Kishore, D. Mysaiah, H.V.S. Satyanarayan and T. Seshunarayana*  
*National Geophysical Research Institute, Council of scientific and Industrial Research, Uppal*  
*Road, Hyderabad 500007, India*

\*Email: [strupiti\\_13@yahoo.com](mailto:strupiti_13@yahoo.com)

### **Abstract**

The Seismic refraction method is helpful in understanding the near-surface geological conditions. For civil engineering constructions like dams, tunnels, etc., an analysis of near-surface geologic conditions are basic requirement. This technique effectively provides clues to the near-surface distribution of rocks and soils, and their physical properties. Seismic refraction was conducted along 5 km length for a tunneling purpose near Koduru district of Andhra Pradesh. The data was acquired at 47 profiles laid in N-S direction. The data processing was done by combining the profiles which are overlapped by 5 m to get the detailed information. The area is surrounded by a gneissic and granitic formation, Nallamalai formations (shales) of the Cuddapah basin, and by several lineaments/faults. Our results revealed a three-layered case; the first layer is related to soil cover with maximum P-wave velocity ( $V_P$ ) of 600 m/s. The second layer  $V_P$  in the range of 1300 - 1900 m/s pertains to weathered sedimentary rock and the bottom layer which has  $V_P$  in between 2100 and 3500 m/s (in some cases it exceeds 5000 m/s). The bottom layer is interpreted as semi-weathered basement rock composed of arenaceous and argillaceous rocks. Our study shows that the seismic refraction method is a less expensive and accurate technique, and it has demarcated the spatial extent of soil cover, weathered, semi-weathered and hard rocks in the near-surface.

**Keywords:** Tunnel; seismic refraction; velocity; civil engineering constructions.

### **1 Introduction**

Tunnel construction is an important task, but the nature of all kinds of geological problems will have a high impact on them. In order to ensure the safety and the stability of tunnel, geophysical investigations need to be carried out to understand the geological structure. From the civil engineering point of view, shallow seismic refraction has been used to study the bedrock foundation properties in road tunneling, dam sites, quarries, hydroelectric power plants, subway constructions, nuclear power plants, etc. In these types of surveys, one needs to understand the detailed near-surface layers to explore some specific objectives like faults, cracks, caves, and aquifers. Due to the presence of hidden geological features such as faults/cavity the structures can experience damage to the civil engineering constructions. Of all the geophysical methods, the electrical resistivity and the seismic refraction methods have proved very useful in foundation studies (Whiteley and Eccleston 2006).

These have many advantages over the other shallow techniques as it is feasible to determine subsurface structure (seismic velocity) with sufficient resolution and accuracy. Similar studies were carried out in the Jabalpur area (Seshunarayana et al. 2002), and in Gujarat (Rastogi et al. 2011, Sairam et al. 2011, Sairam et al. 2018, Sairam et al. 2019) for site characterization studies and to estimate the bedrock depth. (Sundararajan et al. 2019) has conducted this type of surveys in Oman for the bedrock studies. The present study is aimed at determining the overburden depth and bedrock depth for the tunnel alignment in Andhra Pradesh. Seismic velocities can assist in the interpretation of geological layers as well as determining the depth to the bedrock.

## Geology:

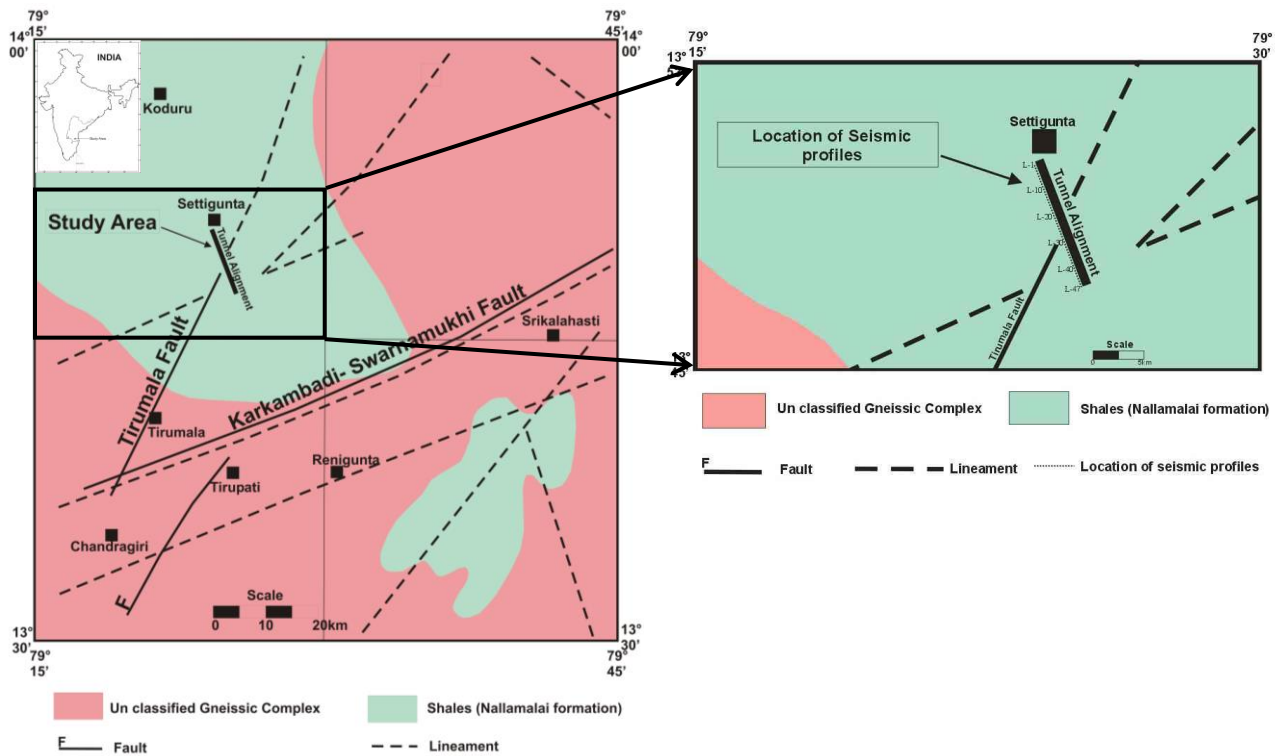


**Fig. 1:** Geology map of the study area. Source: Dasgupta et al. Seismotectonic Atlas and its environs, 2000

The study area is at the tip of the mid to late Proterozoic Cuddapah Basin (Mallikarjuna Rao et al. 1995). The Bairenkonda and Cumbum formations of the Nallamalai Group of the Cuddapah Super Group are exposed in the Koduru-Kadapa area as shown in Fig. 1. The Bairenkonda formation is predominantly an arenaceous unit with subordinate shale/phyllite. The Cumbum formation is dominated by argillaceous phyllite-shale/slate succession with intercalations of quartzite, calcareous shale, tuffs, and dolomite. Some thick bands of quartzite are exposed in the vicinity of the alignments. Only the siltstone, quartzite, and dolomite bands are more resistant to weathering. Quartzite with intermittent slates/ phyllites is exposed and is moderately hard and has well-developed strike joints

The slates/ phyllites are likely to be soft due to a higher degree of weathering and alteration. The beds trend NNW-SSE with moderate to steep dip towards east. Bedding joints are very common. They are closely spaced in all types of rocks including the quartzite bands. The study area is encountered with three faults/lineaments (Fig.1 after [Seismotectonic atlas of India and its environs, Dasgupta et al. 2000](#)) and surrounded by several NE-SW trending lineaments/faults. The survey was conducted to find any structural disturbances within the bedrock for the construction of the tunnel.

## **2 Data Acquisition & Processing**

The seismic refraction survey was conducted at 47 profiles laid in N-S direction along the tunnel and are named as L1, L2.....L47. For some profiles, the data was acquired by taking offsets from the proposed line because the survey area was covered with agriculture crops. Data were obtained by using 24 channels spread (Fig. 2a) of 4.5 Hz geophones with sampling interval of 0.25 ms. Record length was 512 ms and geophones were placed at 5 m interval. The spread length of each profile was 115 m. A 15 kg hammer was used as energy source for the present study. Based on local geology, expected thickness of the weathered formation is about 15-25 m and our target depth of investigation is about 40 m. Five to ten hammer blows were used on a strike plate to improve the coupling of energy from the hammer to the soil. A 24 Channel seismic data acquisition system was used. First breaks were picked from the time traces recorded for each shot point position as shown in the Fig. 2b, and travel-time diagrams were generated. The data was acquired with an overlap of 15 m along the 5 km length and it was processed by combining the profiles with minimum offsets as shown in Figs. 3 and 4. The data of two profiles with high velocity third layer and perpendicular to the main alignment are shown in Figs. 5 and 6. Hence, they are interpreted and presented separately. Finally, a single image was generated for a total of 5 km length and presented in Fig. 7 for a better understanding of the geological layers.

The Time-Term inversion method, a standard inversion iterative method is a linear Least-Squares approach to determine the best discrete-layer solution to the data set ([Bath 1978](#)). The time term inversion technique is applied to the travel-time diagram to calculate the seismic velocities of the different layers and the depths of the layers. It is a simple travel-time inversion method developed by [Scheidegger and Willmore \(1957\)](#) and was widely used for seismic refraction crustal studies in the 1960–70s ([Willmore and Bancroft 1960](#); [Berry and West 1966](#); [Meru, 1966](#); [Smith et al. 1966](#); [Yoshii and Asano 1972](#)). This method has several advantages in spite of its crude travel-time approximation. The first one is the computational stability. The second advantage is the computational efficiency due to the linear equations. This method is quick and is convenient to estimate the refractor depth. The inversion error was less than 1.5 ms. The time-term method is based on a few simple assumptions like discrete constant velocity layers as well as a horizontal refractor.

### **3 Results & Discussions**

The travel-time curves and the depth sections are generated for all the 47 profiles but the few depth sections are presented as example. The interpretation of the combined profiles are shown in Figs. 3a and 3b (profiles L4-L8) as travel-time curves and depth section respectively. Figs. 4a, 4b (profiles L9-L14) as travel-time curves and depth section respectively. Figs. 5 and 6 represent the depth sections of profiles L24 and L43-L46. The velocities of all the profiles are given in Table 1. A three-layered structure of the subsurface is observed on all profiles. Fig. 3b shows the depth section from 500m to 1015 m length, which covers a distance of 515 m. The first layer with a  $V_p \sim 500$  m/s pertaining to soil cover. The thickness of this layer varies from 2 m to 3 m. The second layer with  $V_p \sim 1620$  m/s and thickness varying between 12 m and 14 m, indicates weathered rock. The third layer with  $V_p \sim 2330$  m/s, indicates shale/phyllite. Fig. 4b shows the depth section from 1000 m to 1615 m length, which covers a distance of 615 m. The first layer with  $V_p \sim 550$  m/s, pertaining to soil cover. The thickness of this layer varies from 2 m to 3 m. The second layer with  $V_p \sim 1690$  m/s and thickness varying between 18 m and 20 m, indicates weathered rock. The third layer with  $V_p \sim 2160$  m/s, indicates shale/phyllite. Fig. 5 shows the depth section obtained perpendicularly from the mainline covering a distance of 115 m. The first layer with  $V_p \sim 280$  m/s pertaining to soil cover. The thickness of this layer varies from 2 m to 3 m. The second layer with  $V_p \sim 3510$  m/s and thickness varying between 8 m and 12 m, indicates weathered rock. The third layer with  $V_p \sim 5010$  m/s, indicates hard rock. Fig. 6 shows the depth section obtained from 4600 m-5015 m covering a distance of 415 m. The first layer with  $V_p \sim 490$  m/s pertaining to soil cover. The thickness of this layer varies from 2 m and 3 m. The second layer with  $V_p \sim 1610$  m/s and thickness varying between 8 m and 12 m, indicates weathered rock. The third layer with  $V_p \sim 2360$  m/s, indicates hard rock. The joint interpretation of consecutive profiles provides velocities and depths for the detailed characterization of rock types (Table 1).

The obtained velocities of 2000-3500m/s below 20m depth may be attributed to the semi-weathered shale formations. The first layer is related to soil cover with  $V_p$  in the range of 350 - 600 m/s and bearing thickness of about 2 -3 m. The second layer with  $V_p$  in the range of 1300 -1900 m/s, pertains to weathered sedimentary rock with the thickness of about 15 -25, m and the bottom layer has the  $V_p$  in the range of 2100 - 3500 m/s, and in some cases, it exceeds 5000 m/s indicating the presence of hard siltstone/quartzite. This layer is interpreted as semi-weathered basement material, composed of arenaceous and argillaceous rocks. Thus, from the above studies, it is concluded that the top 20 m is a weathered formation, and it is clearly seen that below 20 m there is an semi-weathered formation. Tuffaceous beds can be somewhat altered at depths exceeding 20 m. Considering the demand in investigations for complex geological features, the method presented here can play a very important role in identifying the depth to bedrock, etc. It can be concluded that the study area consists of weathered formation up to top 20 m-25 m depth, and below 25 m depth it is semi-weathered formations. The results revealed that there are no structural disturbances within the bedrock and the obtained velocities are in good agreement with the local geology i.e., shales.

### Acknowledgements

The authors are grateful to Dr. V. M. Tiwari, Director, CSIR-NGRI for his kind permission to publish this paper. They wish to thank V. V. Ramana Murthy, P. Prabhakar Prasad and the entire erstwhile engineering geophysics group for their help during the field data acquisition. The authors are thankful to the reviewers for their suggestions in improving the manuscript. The first author is grateful to CSIR for sanction of CSIR-RA fellowship.

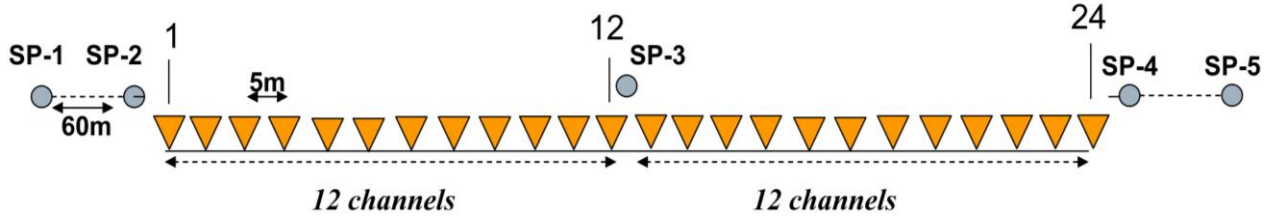


**Fig. 2a:** Shows the collection of data in the field using five shot point method

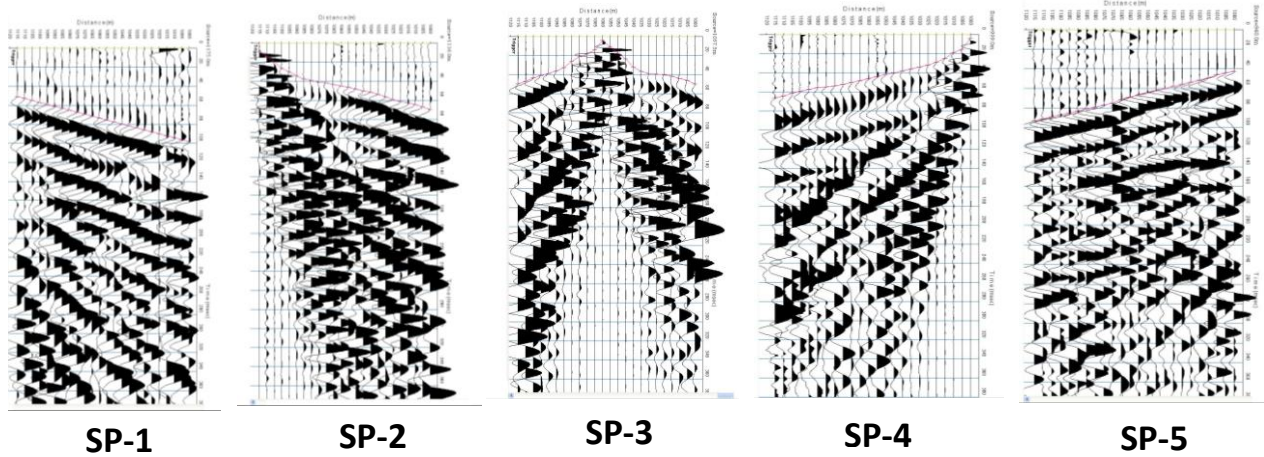


**Fig.2b:** Shows the records obtained during data collection i.e., from SP1, SP2, SP3, SP4 and SP5



*Seismic refraction of bedrock for civil engineering constructions*

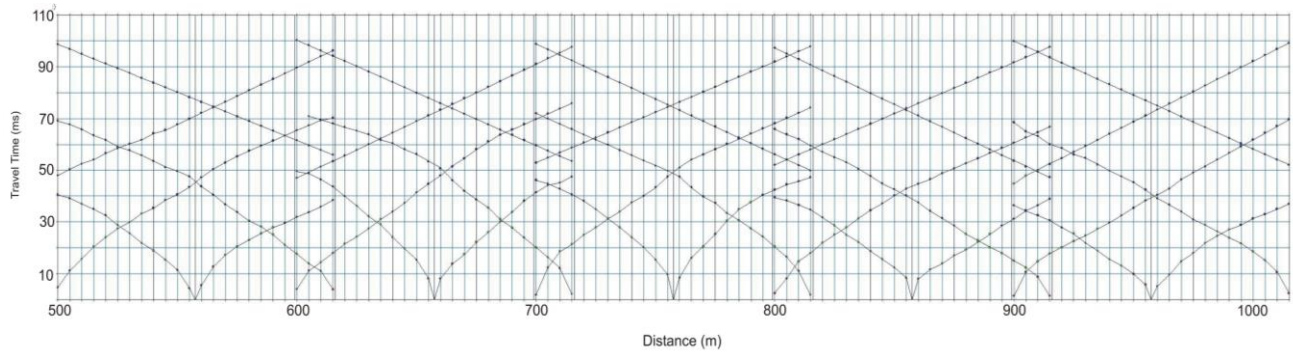


Fig. 3a: Travel time distance graph of 515 m profile

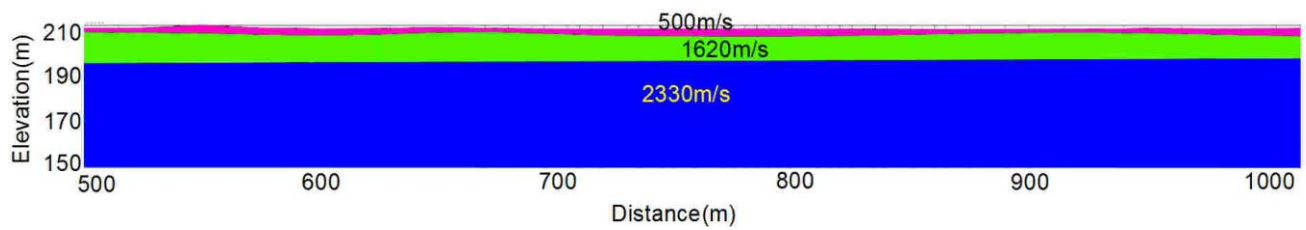


Fig. 3b: The depth section showing the three-layer case covering a distance of 515m

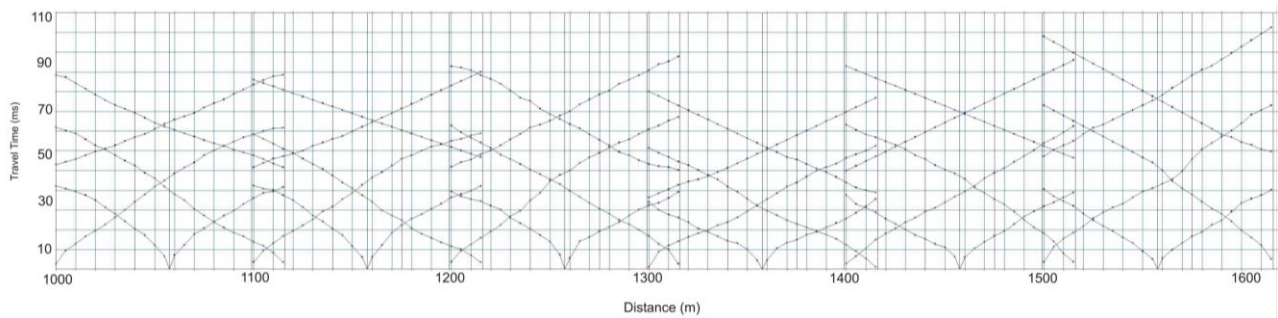


Fig. 4a: Travel time distance graph

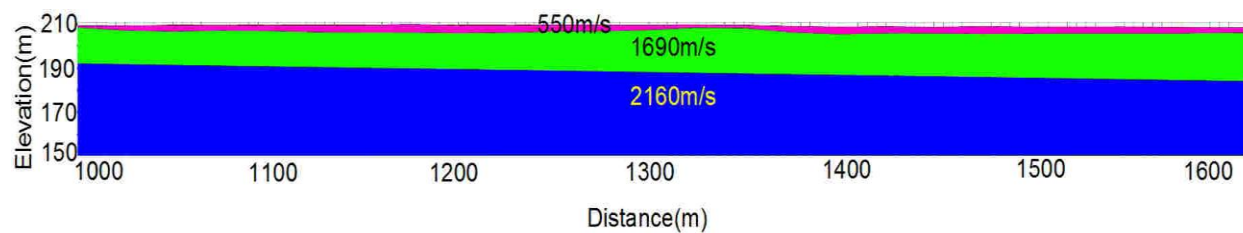


Fig. 4b: Depth section covering a distance of 615 m.

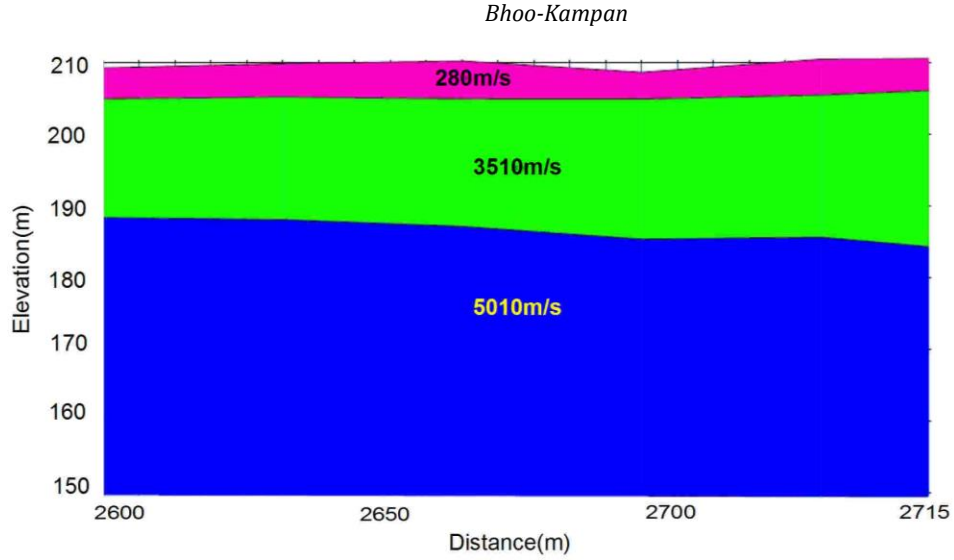


Fig. 5: Depth section with high third layer velocity of  $V_P$  of 5010m/s.

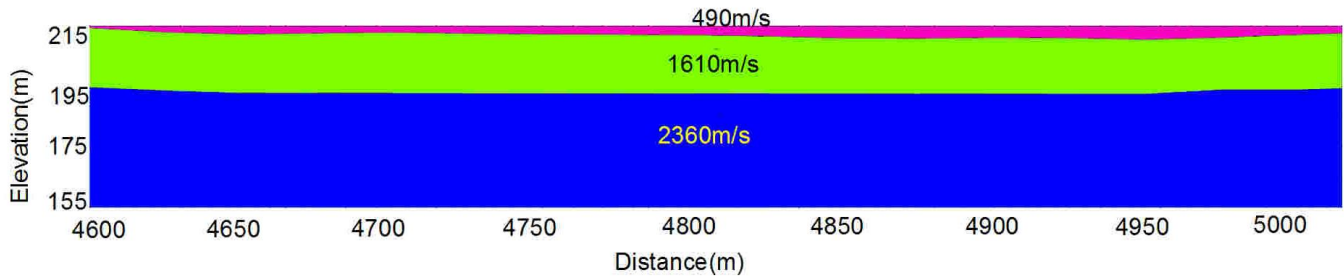
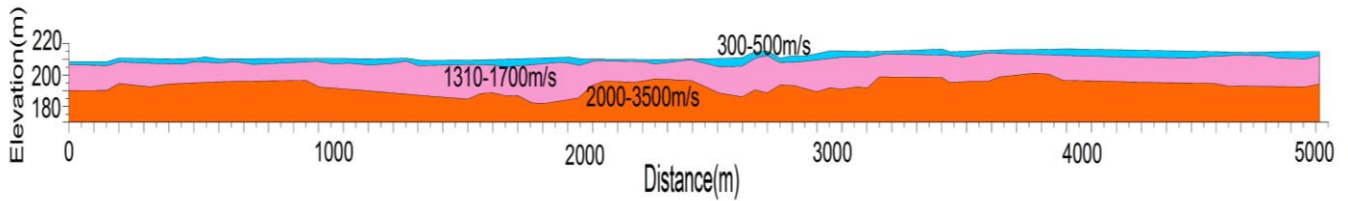


Fig. 6: Cross section for total 5 line kilometres profile at Koduru region



**Fig. 7:** Sketch of the combination of all the 47 profiles covering a distance of 5 Km showing the three layers. The first layer indicates soil cover represented in blue color. The thickness of this layer varies from 2 m to 4 m. The second layer pertains to weathered sedimentary rocks represented in pink color. The bottom layer, represented in red color is interpreted to be semi-weathered basement rocks, composed of arenaceous and argillaceous rocks

Table 1: The result of combined and individual profiles.

SN	Profiles	V <sub>P1</sub> (m/s)	V <sub>P2</sub> (m/s)	V <sub>P3</sub> (m/s)
1.	L31, L32	460	1700	2330
2.	L1, L2, L3	490	1570	2170
3.	L4, L5, L6, L7, L8	500	1620	2330
4.	L9, L10, L11, L12, L13, L14	550	1690	2160
5.	L17, L18	380	1450	2040
6.	L20, L21, L22, L23	340	1310	2970
7.	L26, L27	320	1470	2470
8.	L33, L34, L35	390	1410	2100
9.	L36, L37, L38, L39, L40	310	1510	2410
10.	L41, L42	340	1510	2140
11.	L43, L44, L45, L46	490	1610	2360
12.	L15	390	1590	2030
13.	L24	280	3510	5010
14.	L29	290	1690	3490
15.	L30	280	1990	3210
16.	L16	410	1120	2090
17.	L19	440	1690	2290
18.	L25	270	1770	2900
19.	L28	350	1880	3100
20.	L47	390	1520	2630

## References

1. Bath, M. (1978). An analysis of the time term method in refraction seismology, *Tectonophysics*, v.51, pp: 155-169
2. Berry, M. J. and West., G. F. (1966). An interpretation of the first arrival data of the Lake Superior experiment by the time-term method, *Bull. Seism. Soc. Am.*, v. 56, pp: 141–171
3. Mallikarjuna Rao, J., Rao, M.N and Wampler, J.M. (1995). Mid-to-late-Proterozoic basin igneous rocks of Cuddapah Basin- their mode of emplacement, petrography, geochemical characteristics and K-Ar ages. Tirupati' 95, Seminar on Cuddapah Basin, *Geol. Soc. India*, Annual Convention, 104
4. Meru, R. F (1966). An iterative method for solving the time-term equations, J. S.Steinhardt and T. J. Smith, Ed., *Geophys. Monogr., Am. Geophys. Union* v.10, pp: 495–497
5. Rastogi, B.K., Singh, A.P., Sairam, B., Jain, S.K., Kaneko, F., Sewago, S., and Matsuo, J. (2011). The possibility of site effects: The Anjar case, following past earthquakes in Gujarat, India. *Seismological Research Letters*, 82(1), 59-68



6. Sairam, B., Rastogi, B.K., Aggarwal, S., Chauhan, M., and Bhonde, U. (2011). Seismic site characterization using Vs30 and site amplification in Gandhinagar region, Gujarat, India. *Current Science*, **100**(5), 754-761
7. Sairam, B., Singh, A. P., Patel, V., Pancholi, V., Chopra, S., Dwivedi, V. K., & Ravi Kumar, M. (2018). Influence of local site effects in the Ahmedabad mega City on the damage due to past earthquakes in northwestern India. *Bulletin of the Seismological Society of America*, **108**(4), 2170-2182.
8. Sairam, B., Singh, A. P., Patel, V., Chopra, S., & Kumar, M. R. (2019). VS30 mapping and site characterization in the seismically active intraplate region of Western India: implications for risk mitigation. *Near Surface Geophysics*, **17**(5), 533-546
9. Scheidegger, A. and Willmore, P. L. (1957). The use of a least square method for the interpretation of data from seismic surveys, *Geophysics*, v. **22**, pp: 9-22
10. Seshunarayana, T., et al. (2002). Report on seismic survey for determination of  $V_p$  and  $V_s$  of shallow subsoil & bedrock depth in Jabalpur area for use in microzonation studies. Tech. Report No: NGRI-2002-Exp-359
11. Smith, T. J., Steinhart, J.S. and Aldrich, L.J. (1966). Lake Superior crustal structure, *J. Geophys. Res.*, v. **71**, pp: 1141-1172
12. Dasgupta, Sujit, Prabhas Pande, Ganguly, D., Iqbal, Z., Sanyal, K., Venkatraman, N.V., Dasgupta, S., Sural, B., Harendranath, L., Mazumdar, K., Sanyal, S., Roy, A., Das, L.K., Misra, P.S., and Harsh Gupta (2000). Seismotectonic Atlas of India and its Environs, *Geological Survey of India*
13. Sundararajan, N., El-Hussain, I., Mohamed, A. M., Deif, A., El-Hady, S., Al-Jabri, K., ... & Al-Wardi, M. (2019). Shear Wave Velocity Characteristics in Parts of Muscat, Sultanate of Oman—A Measure of Earthquake Hazard Assessment. *Journal of the Geological Society of India*, **93**(5), 515-522
14. Whiteley, R. J. and Eccleston, P. J. (2006). Comparison of shallow seismic refraction interpretation methods for regolith mapping. *Exploration Geophysics*, **37**, 340-347
15. Willmore, P. L. and Bancroft, A. M. (1960). The time-term method approach to refraction seismology, *Geophys. J.*, v. **3**, pp: 419-432
16. Yoshii, T. and Asano, S. (1972). Time-term analysis of explosion seismic data, *J. Phys. Earth*, v. **20**, pp: 47-57.